Supporting Information

Synthetic Chemistry and Multifunctionality of Amorphous Ni-MOF-74 Shell on Ni/SiO_2 Hollow Catalyst for Efficient Tandem Reactions

Bowen Li, and Hua Chun Zeng*

Department of Chemical and Biomolecular Engineering, Faculty of Engineering, National University of Singapore, 10 Kent Ridge Crescent, Singapore 119260

* Email: chezhc@nus.edu.sg

Table of Contents

Supporting Figures:

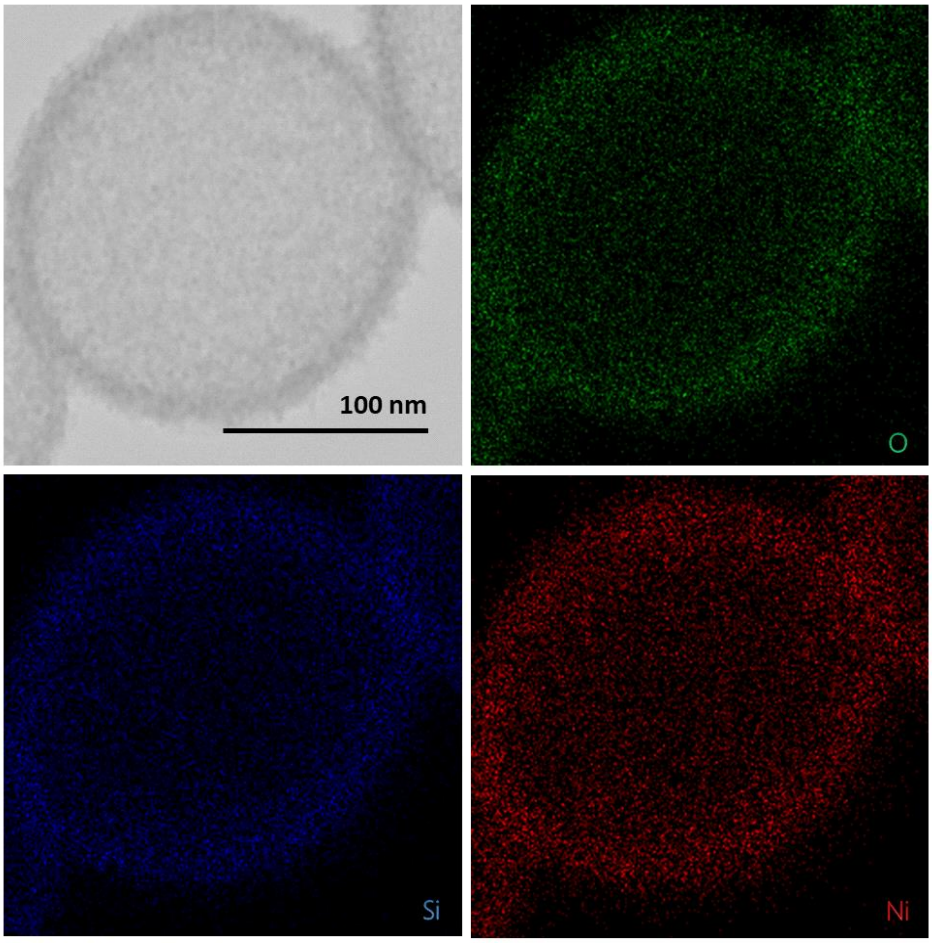

Figure S1. EDX mappings of Ni/SiO_2 hollow sphere.

Comment: As revealed by these EDX mappings, all three elements (O, Si and Ni) were homogeneously distributed across the structure.

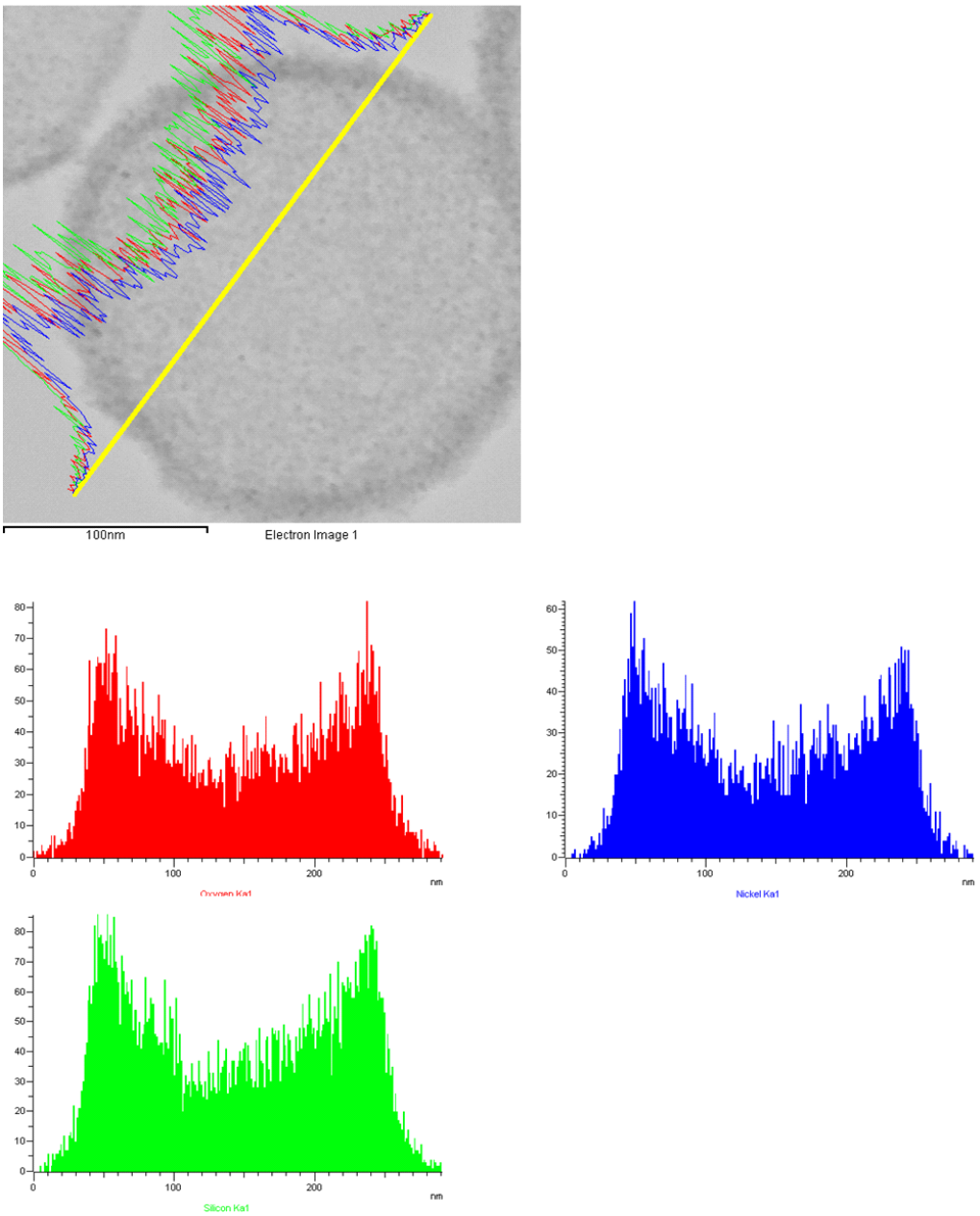

Figure S2. EDX line scans of Ni/SiO_2 hollow sphere.

Comment: For O, Si and Ni, double peaks were observed at the edges of the sphere to illustrate the hollow nature of this structure.

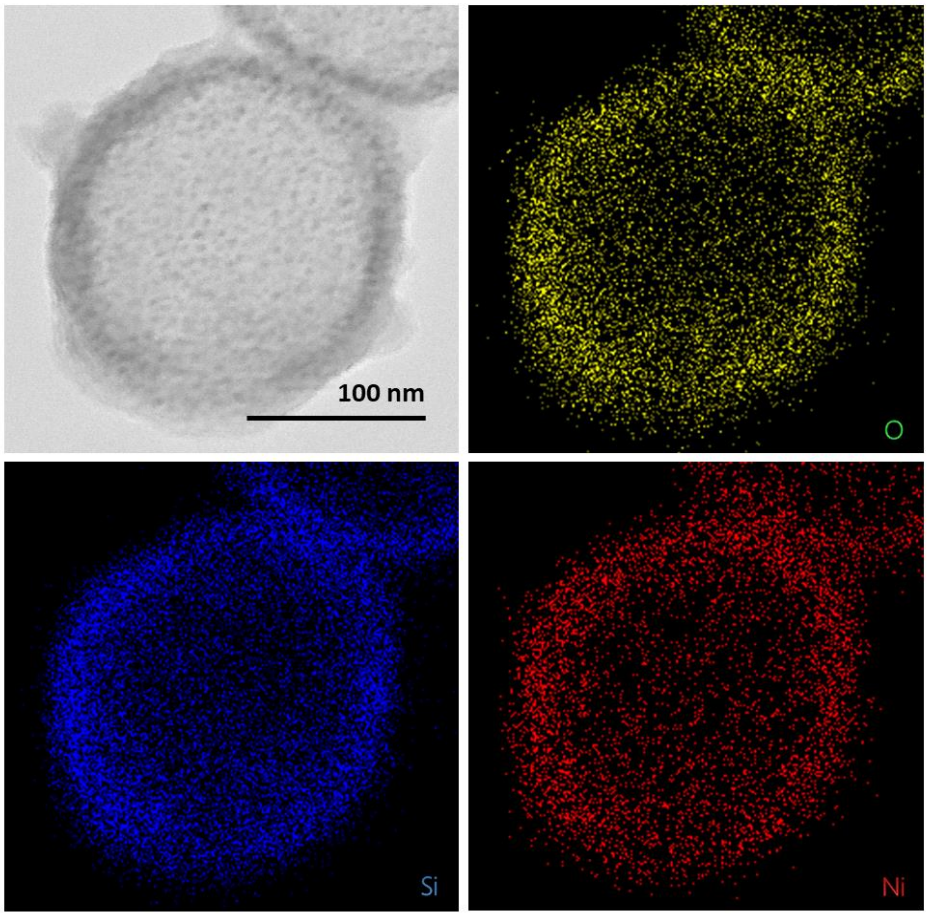

Figure S3. EDX mappings of Ni/SiO_2@a_mNi-MOF-74 (12h) hollow sphere. This sample was prepared by mixing Ni/SiO_2 with H_4DOBDC at 110 °C for 12 h.

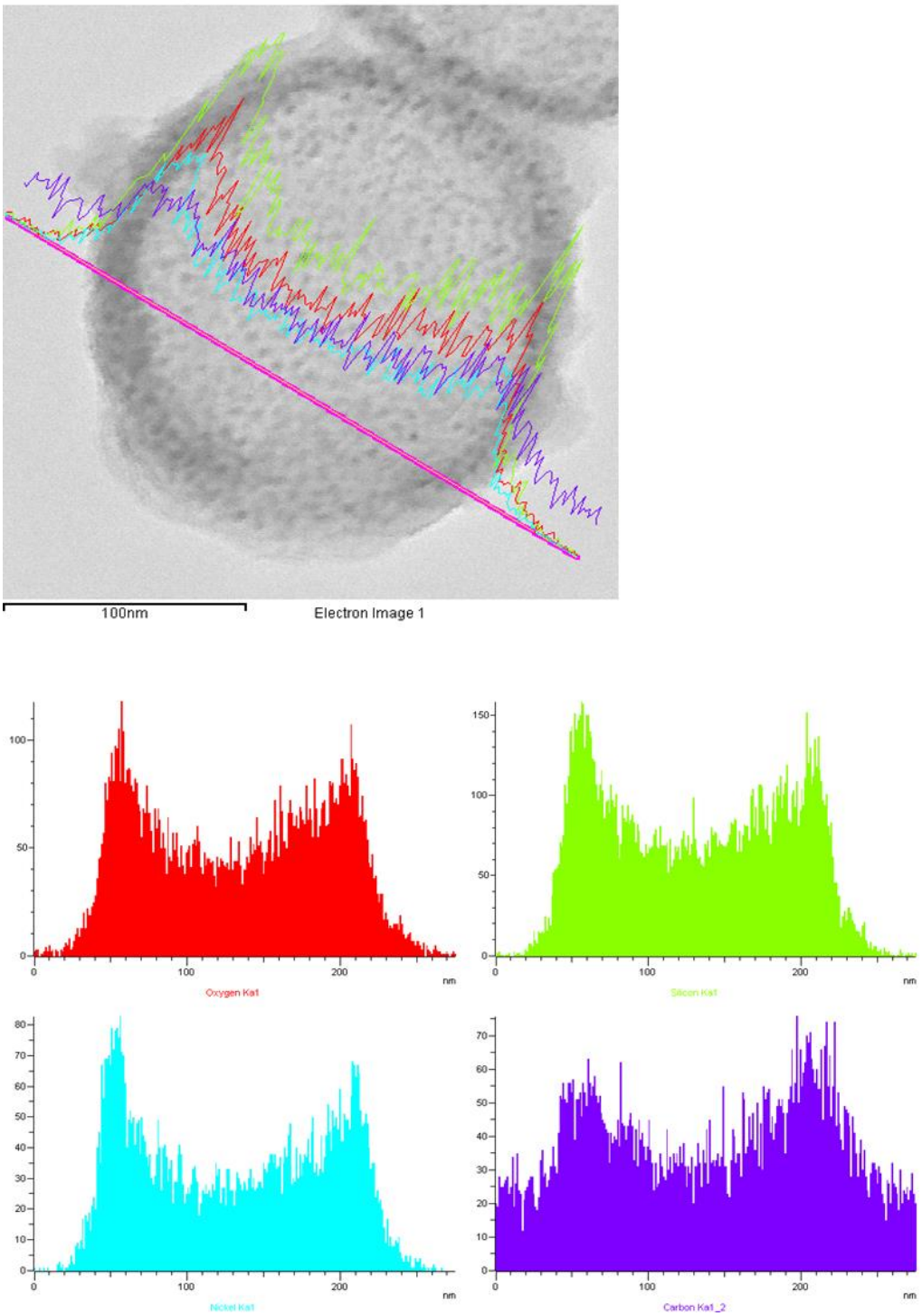

Figure S4. EDX line scans of Ni/SiO_2@a_mNi-MOF-74 (12h) hollow sphere. This sample was prepared by mixing Ni/SiO_2 with H_4DOBDC at 110 °C for 12 h.

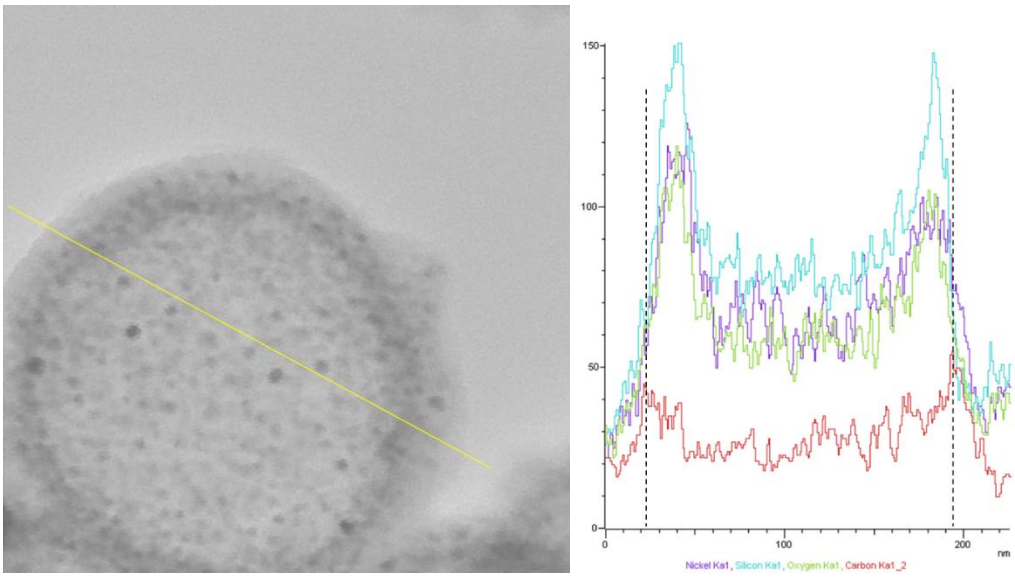

Figure S5. EDX line scans of Ni/SiO_2@a_mNi-MOF-74 (12h) hollow sphere. This sample was prepared by mixing Ni/SiO_2 with H_4DOBDC at 110 °C for 16 h. The peaks of carbon (red line) has shown a clear distinction from those of Si/Ni/O.

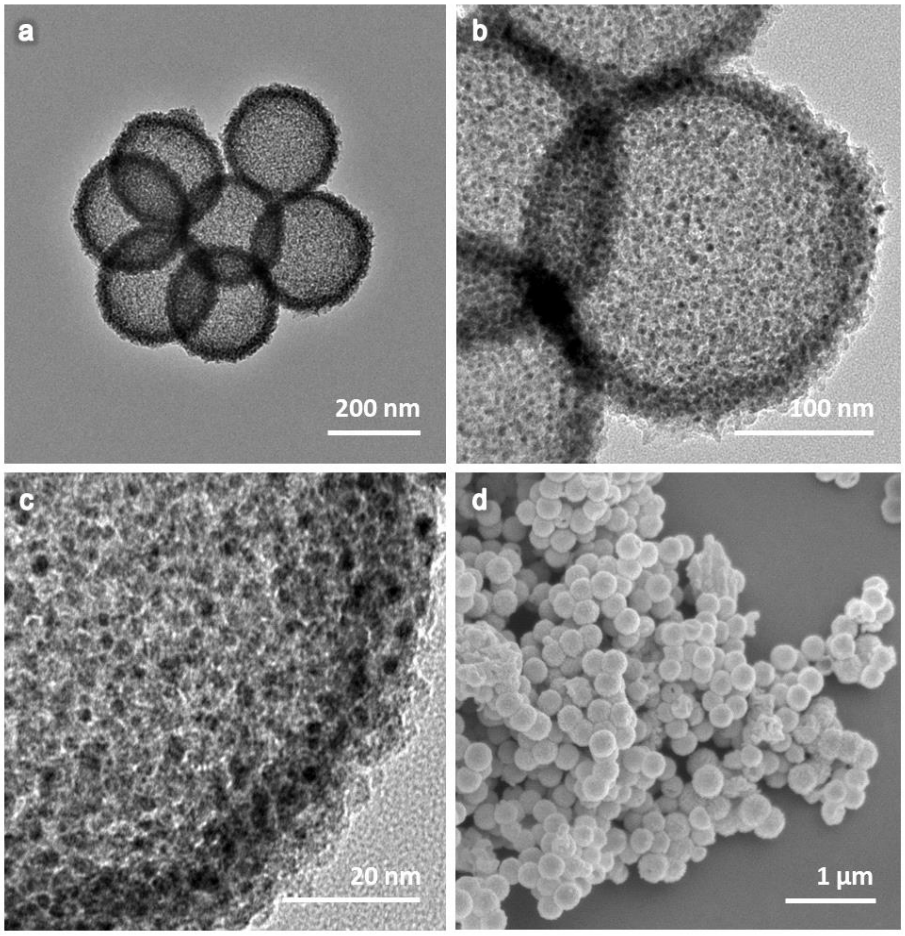

Figure S6. Representative (a-c) TEM and (d) SEM images of Ni/SiO_2@a_mNi-MOF-74 (4h) hollow spheres. This sample was prepared by mixing Ni/SiO_2 with H_4DOBDC at 110 °C for 4 h.

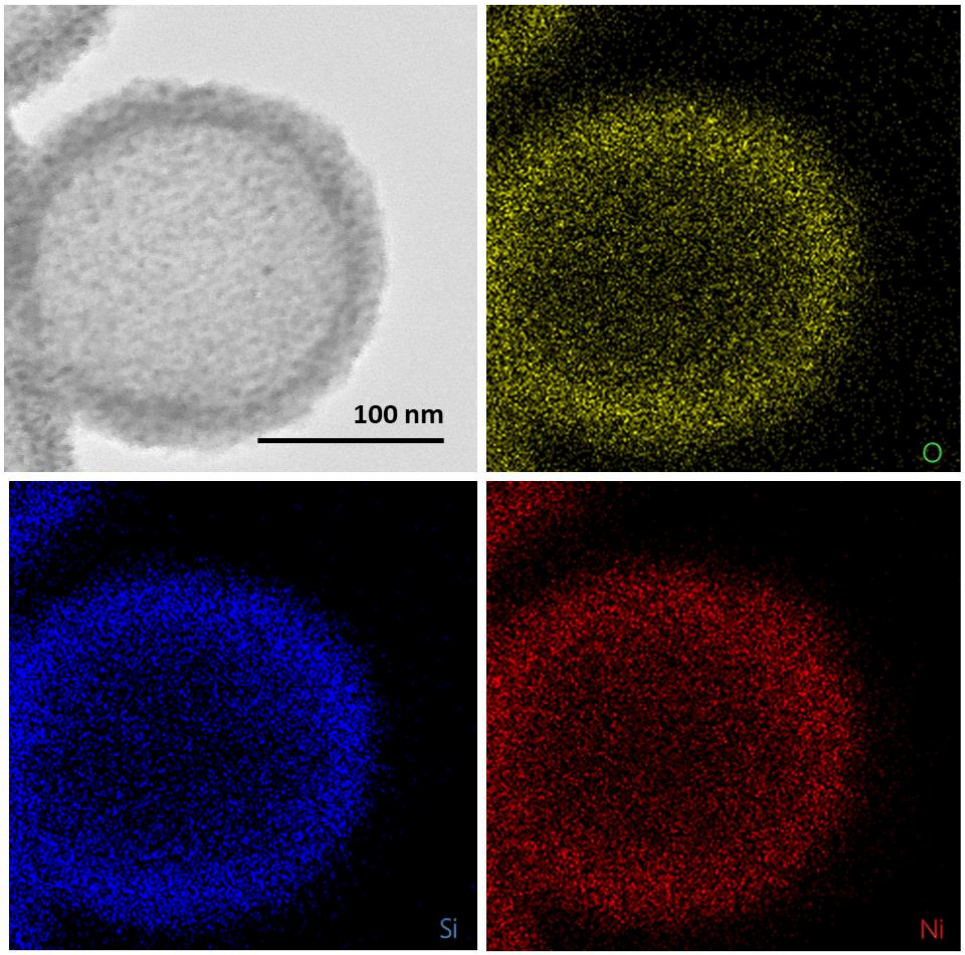

Figure S7. EDX mappings of Ni/SiO_2@a_mNi-MOF-74 (4h) hollow sphere. This sample was prepared by mixing Ni/SiO_2 with H_4DOBDC at 110 °C for 4 h.

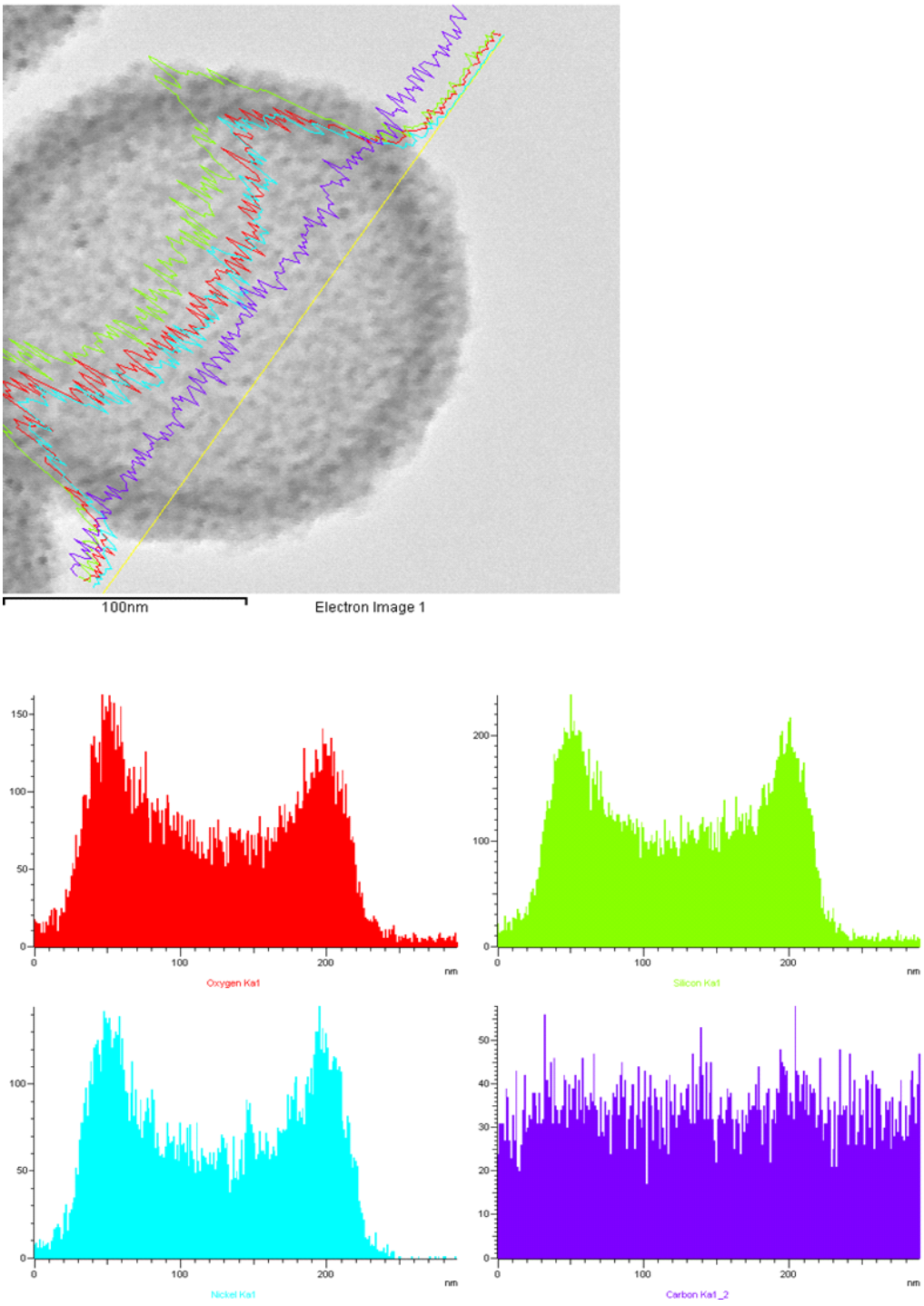

Figure S8. EDX mappings of Ni/SiO_2@a_mNi-MOF-74 (4h) hollow sphere. This sample was prepared by mixing Ni/SiO_2 with H_4DOBDC at 110 °C for 4 h.

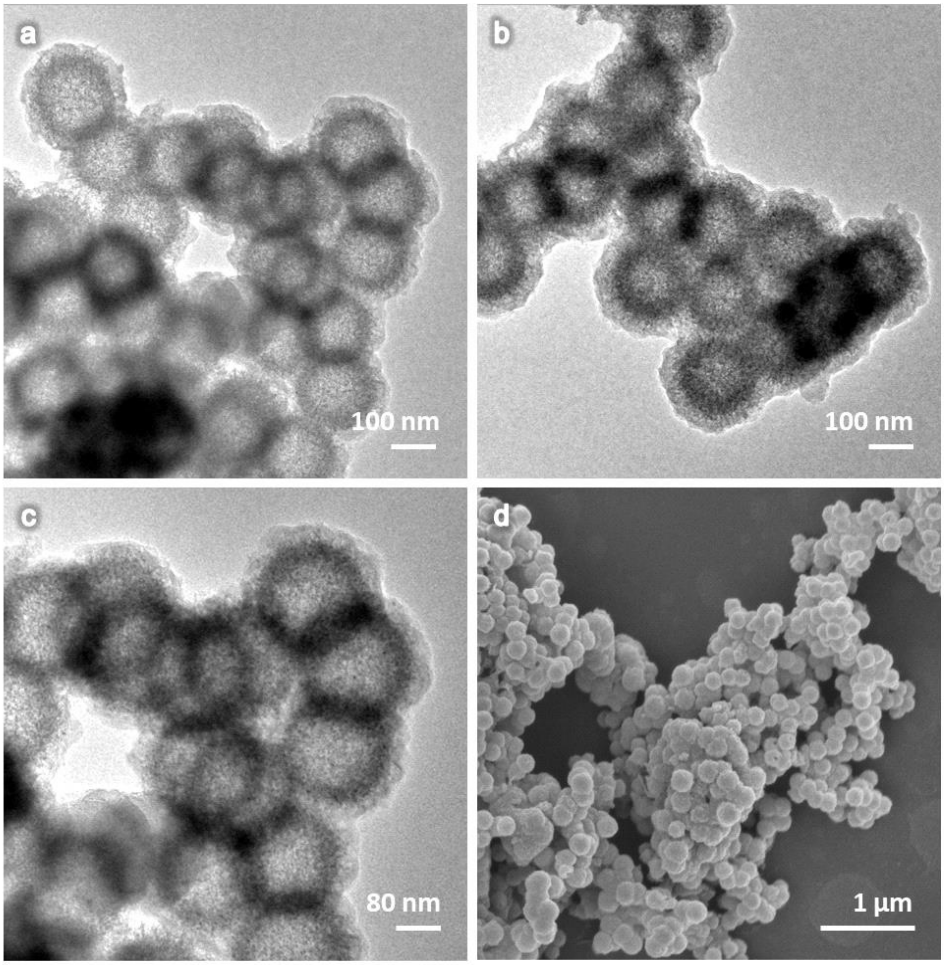

Figure S9. Representative (a-c) TEM and (d) SEM images of Ni/SiO_2@a_mNi-MOF-74 (16h) hollow spheres. This sample was prepared by mixing Ni/SiO_2 with H_4DOBDC at 110 °C for 16 h.

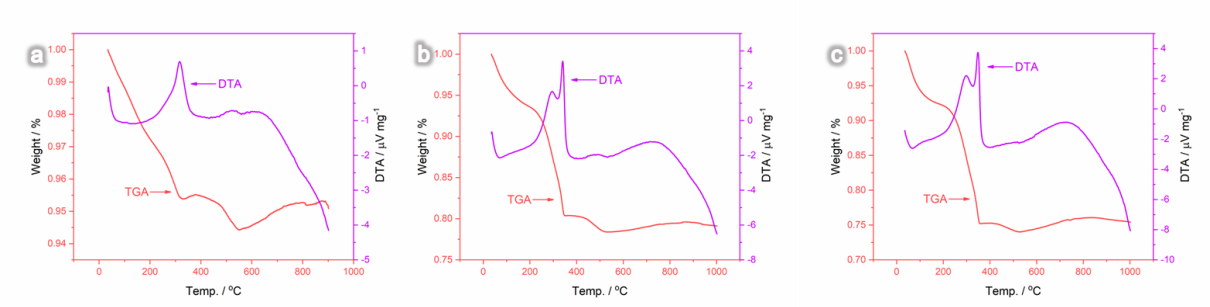

Figure S10. TGA and DTA curves for (a) Ni/SiO_2@a_mNi-MOF-74 (4h) sample, (b) Ni/SiO_2@a_mNi-MOF-74 (12h) sample and (c) Ni/SiO_2@a_mNi-MOF-74 (16h) sample.

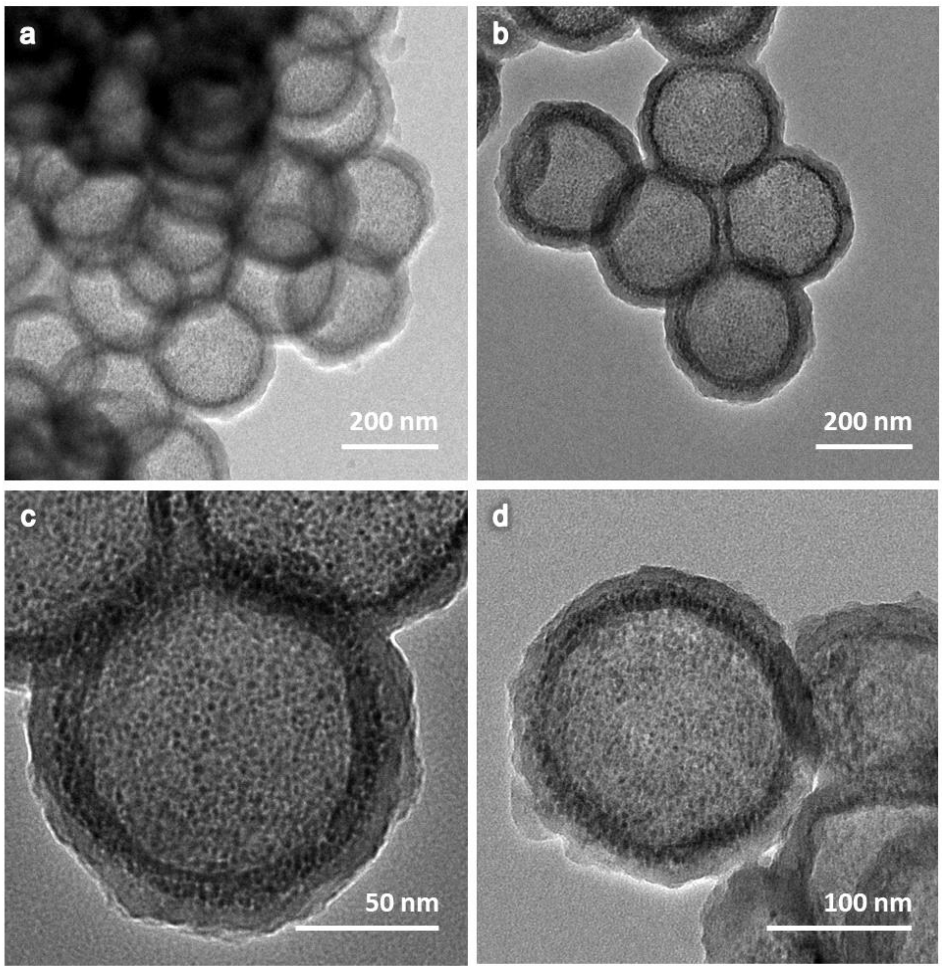

Figure S11. Representative (a-c) TEM and (d) SEM images of Ni/SiO_2@a_mNi-MOF-74 (aged) hollow spheres. This sample was kept in ambient air for 2 days prior to mixing with H_4DOBDC at 110 °C for 12 h.

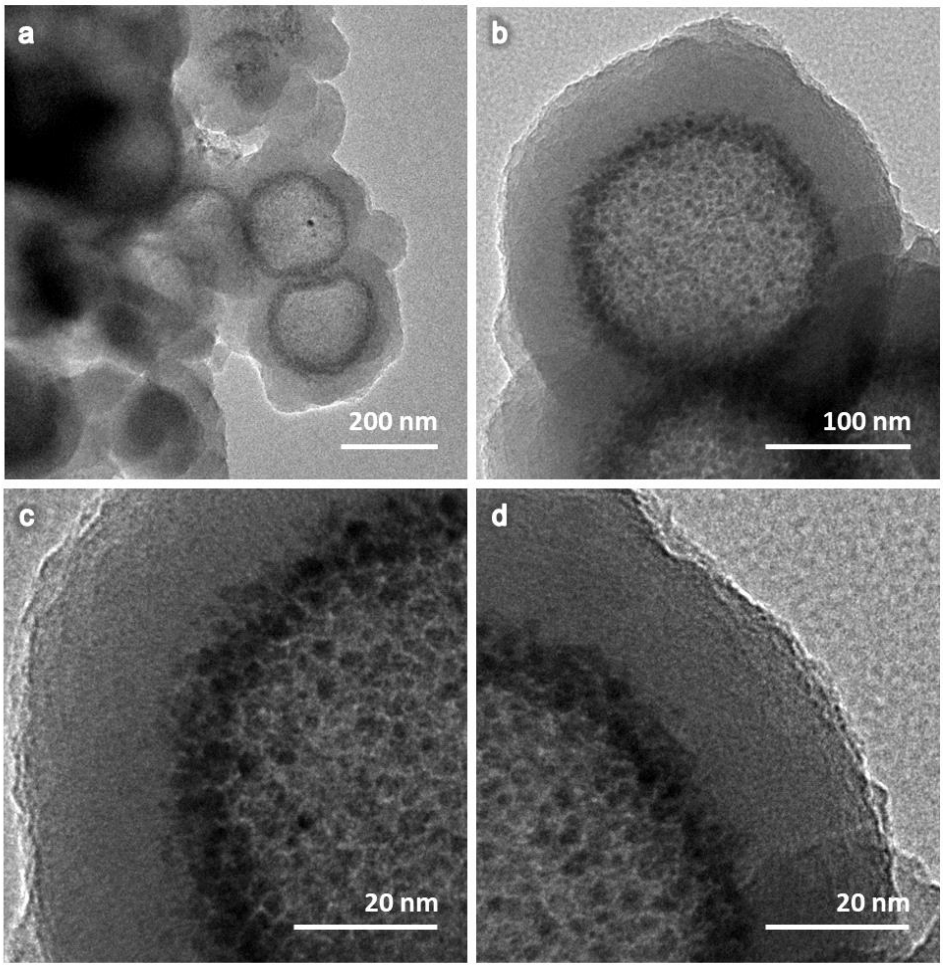

Figure S12. Representative TEM images of Ni/SiO_2@a_mNi-MOF-74 (water) hollow spheres. This sample was prepared by mixing Ni/SiO_2 with H_4DOBDC at 110 °C for 12 h. Additional 4 mL of water was introduced as cosolvent.

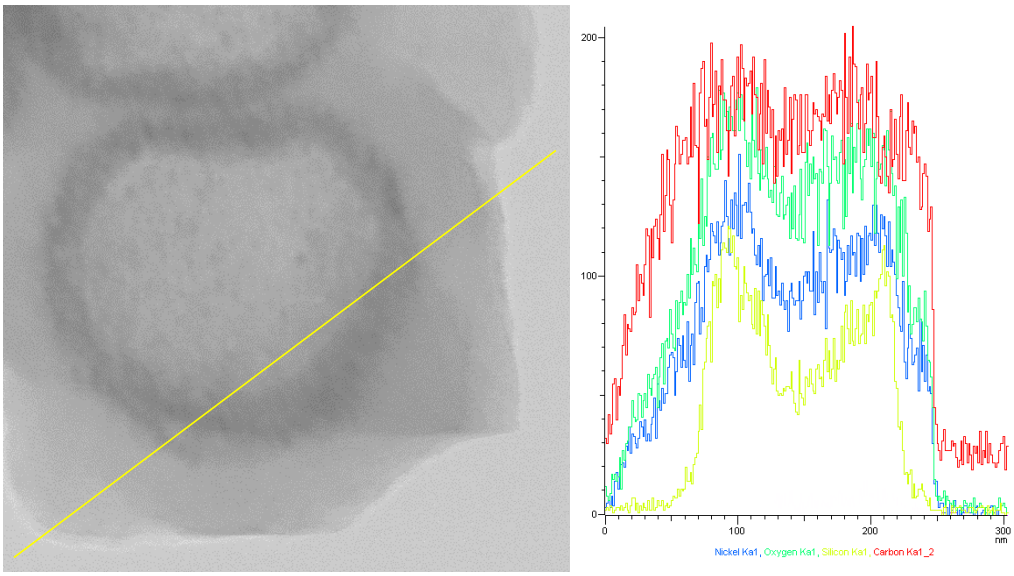

Figure S13. EDX line scans of Ni/SiO_2@a_mNi-MOF-74 (16h) hollow spheres. This sample was prepared by mixing Ni/SiO_2 with H_4DOBDC at 110 °C for 16 h. The peaks of silicon (yellow line) has shown a clear distinction from those of C/Ni/O.

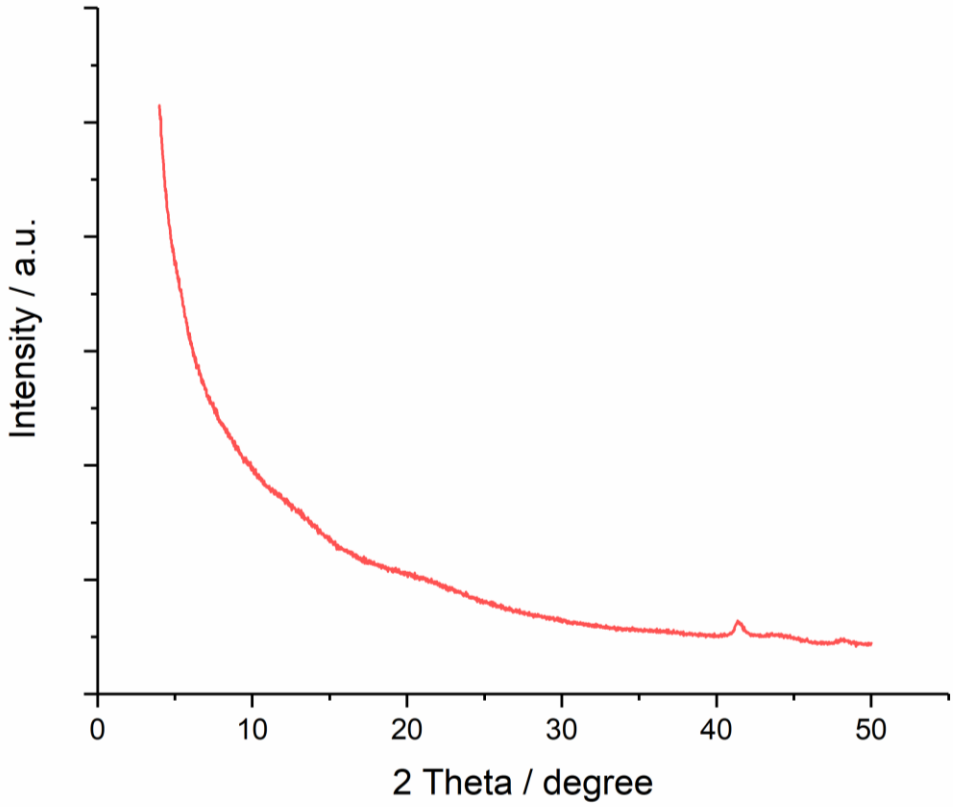

Figure S14. PXRD measurement of Ni/SiO_2@a_mNi-MOF-74 (water) hollow spheres. This sample was prepared by mixing Ni/SiO_2 with H_4DOBDC at 110 °C for 12 h. Additional 4 mL of water was introduced as cosolvent.

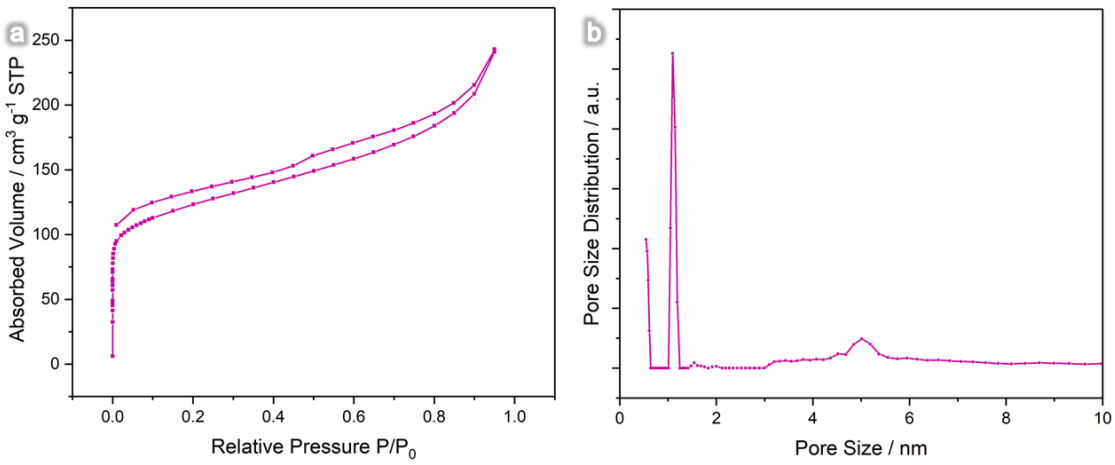

Figure S15. (a) N_2-sorption isotherm and (b) pore size distribution of a_mNi-MOF-74 (water) with thick MOF shell.

Comment: As reflected from the plots, there is a clear type IV isotherm after MOF formation, confirming the existence of mesopores within the newly formed amorphous MOF shell. BET surface area also has measured to be 447.4 m^2/g. From the pore size distribution plot, peak at 1.1 nm can be identified for this Ni/SiO_2@a_mNi-MOF-74 sample, agreeing well with the reported MOF-74 pore dimension. Since this sample is also amorphous, we think it is reasonable to assume that other thinner a_mNi-MOF-74 shells have similar pore size distribution.

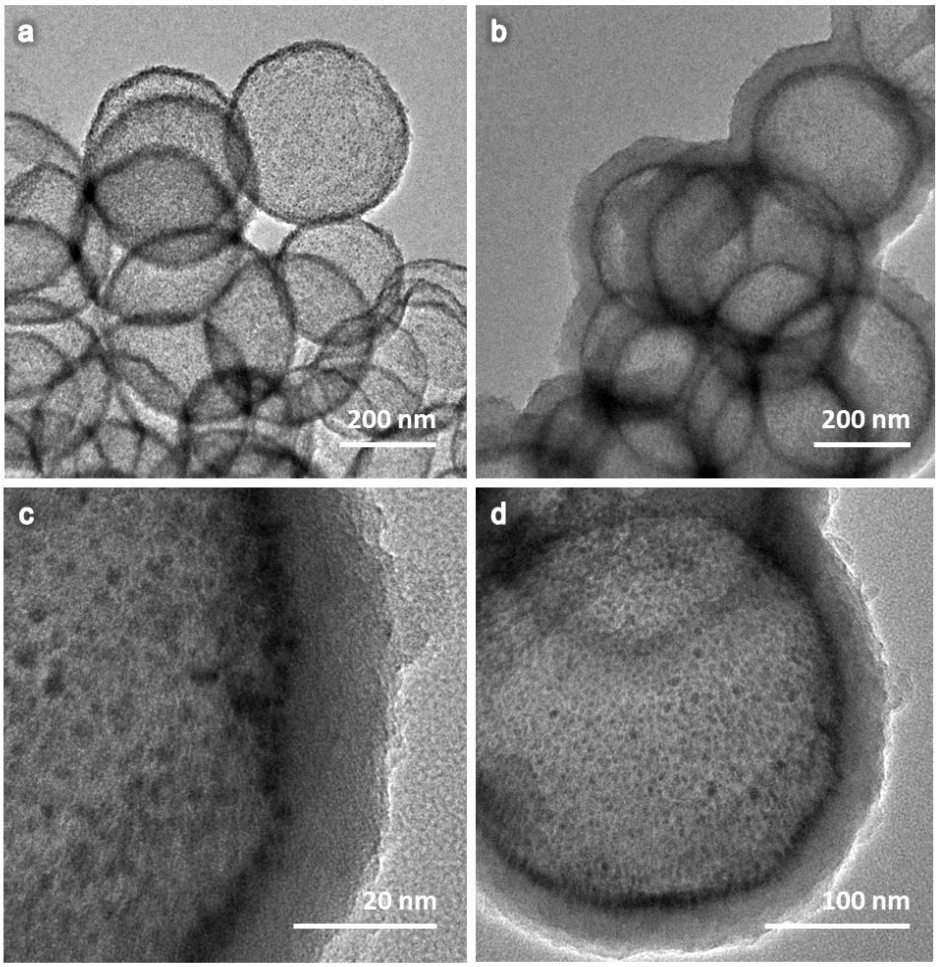

Figure S16. Representative TEM images of Ni/SiO_2@a_mNi-MOF-74 (autoclave) hollow spheres prepared using autoclave without stirring.

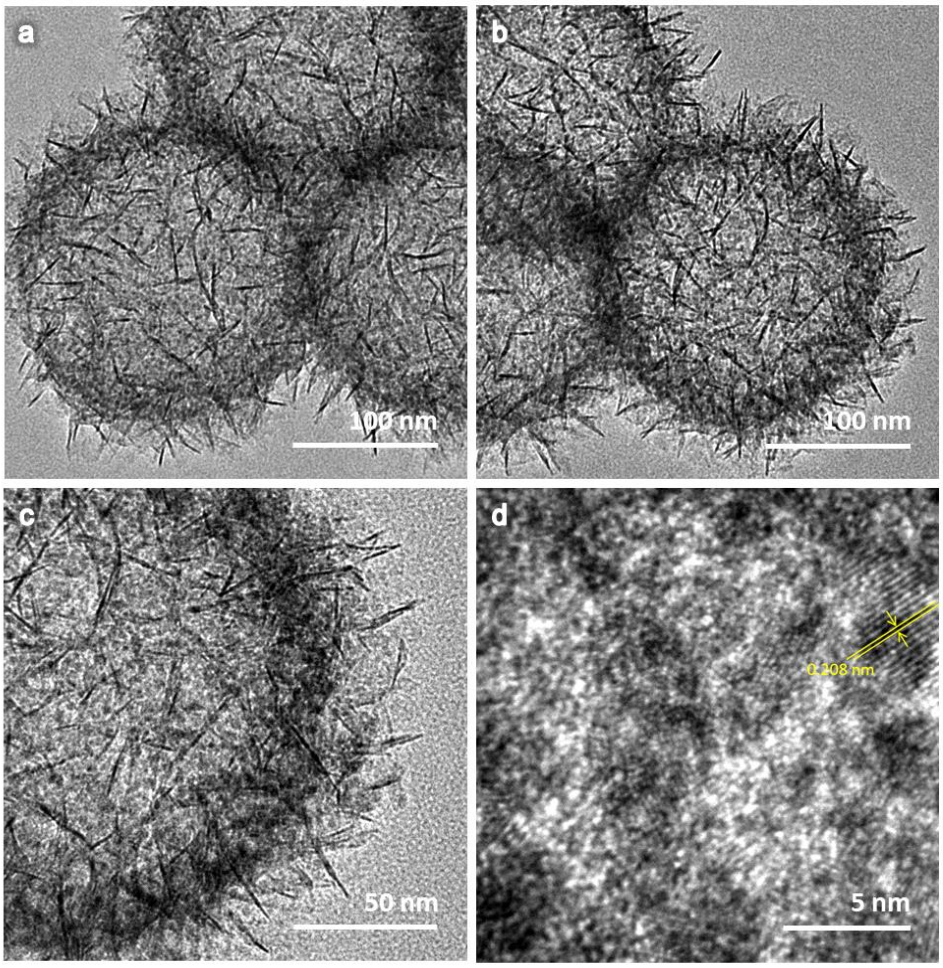

Figure S17. Representative TEM images of Ni/NiSiO hollow spheres prepared by H_2 reduction of NiSiO for 4 h at 500 °C.

Comment: When nickel silicate hollow sphere was reduced for 4 h at 500 °C, the reduction is incomplete, and these reduced Ni NPs could be used as precursors for deposition of Pd via galvanic replacement reaction.

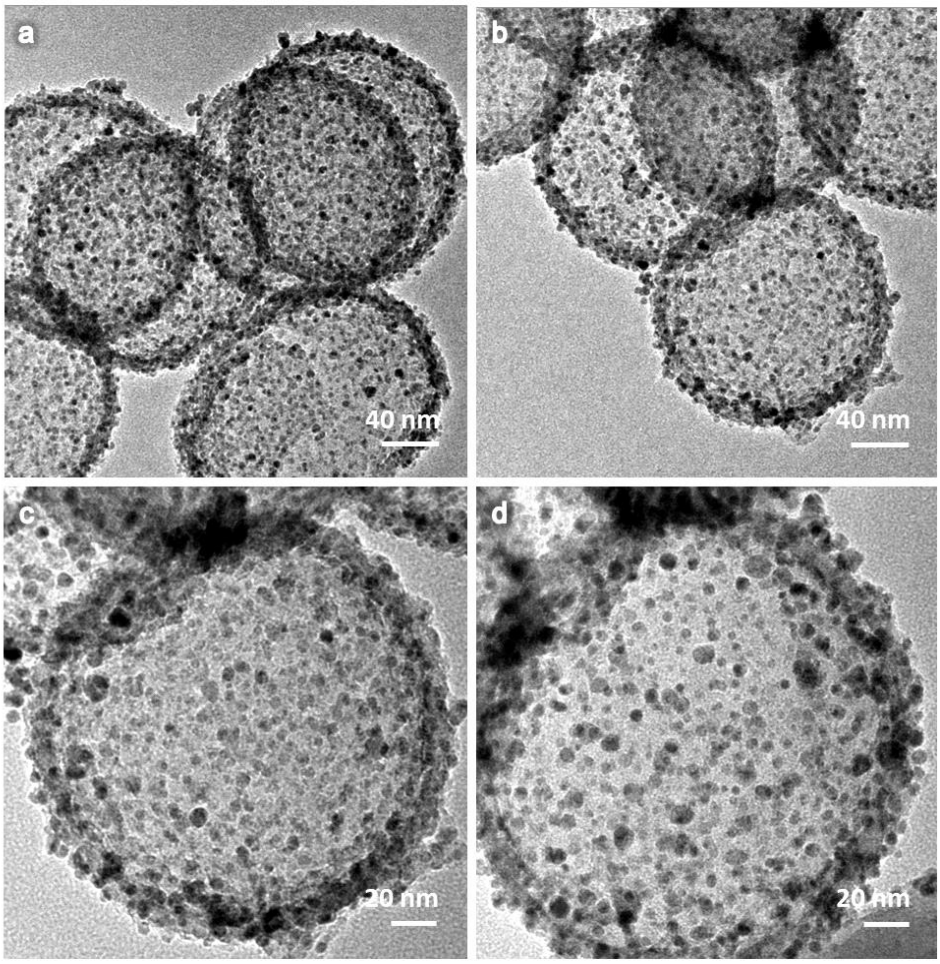

Figure S18. Representative TEM images of NiPd/NiSiO hollow spheres prepared by galvanic replacement without PVP.

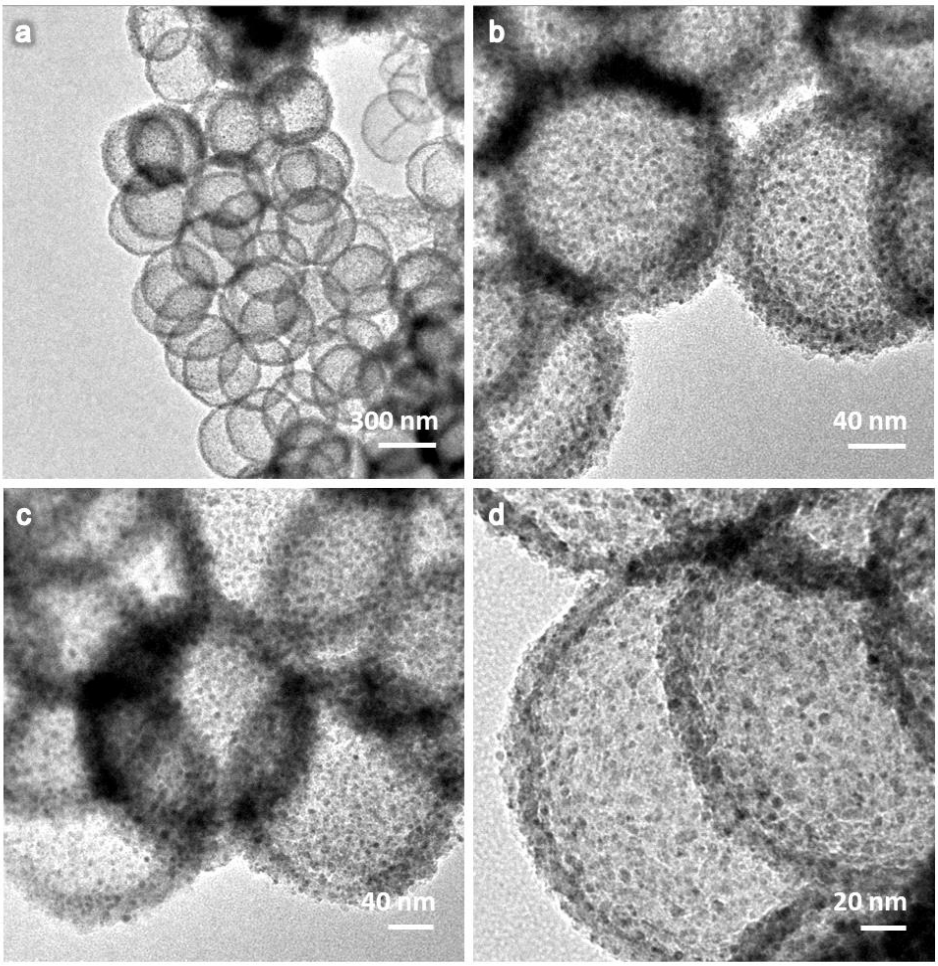

Figure S19. Representative TEM images of NiPd/NiSiO hollow spheres prepared by galvanic replacement with 25 μL of PVP.

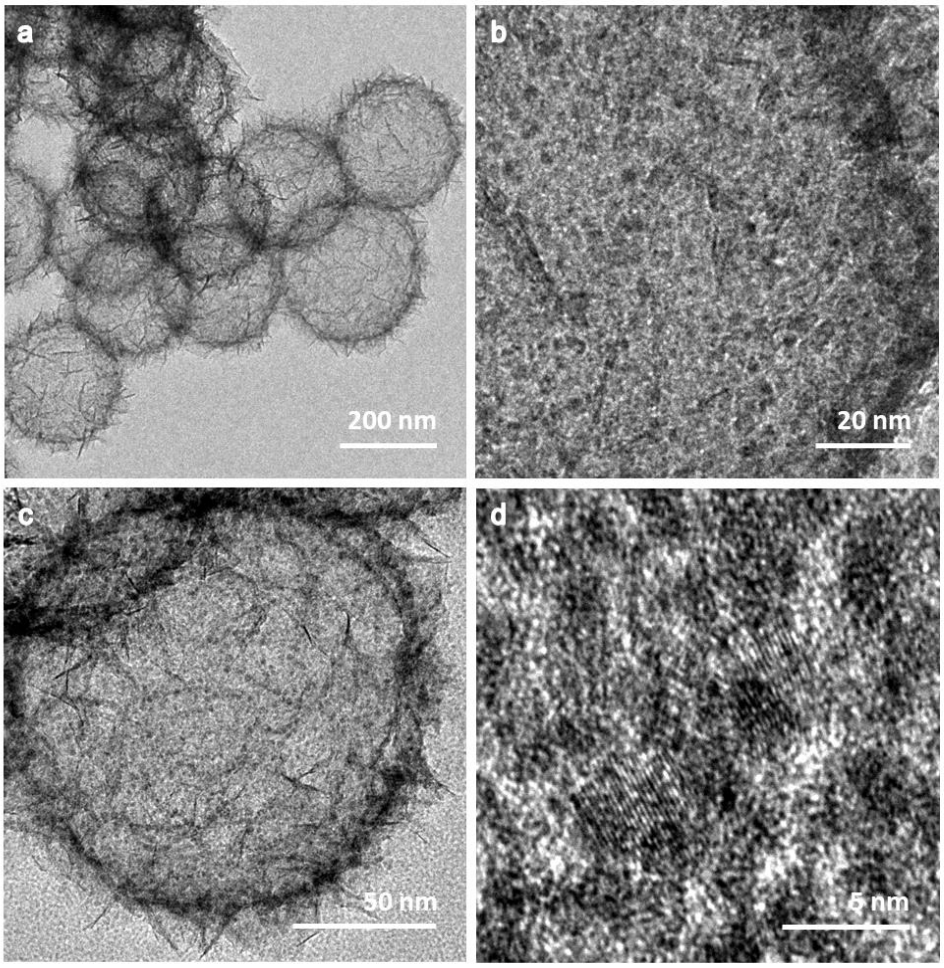

Figure S20. Representative TEM images of NiPd/NiSiO hollow spheres prepared by galvanic replacement with 100 μL of PVP.

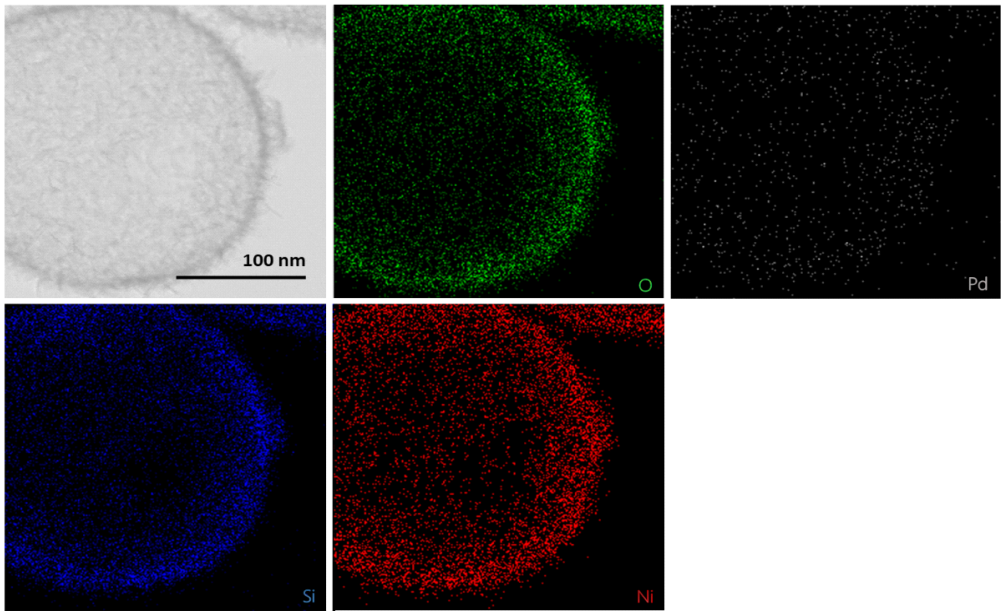

Figure S21. EDX mappings of NiPd/NiSiO hollow sphere prepared by galvanic replacement of Ni/NiSiO with Pd solution and 100 µL of PVP.

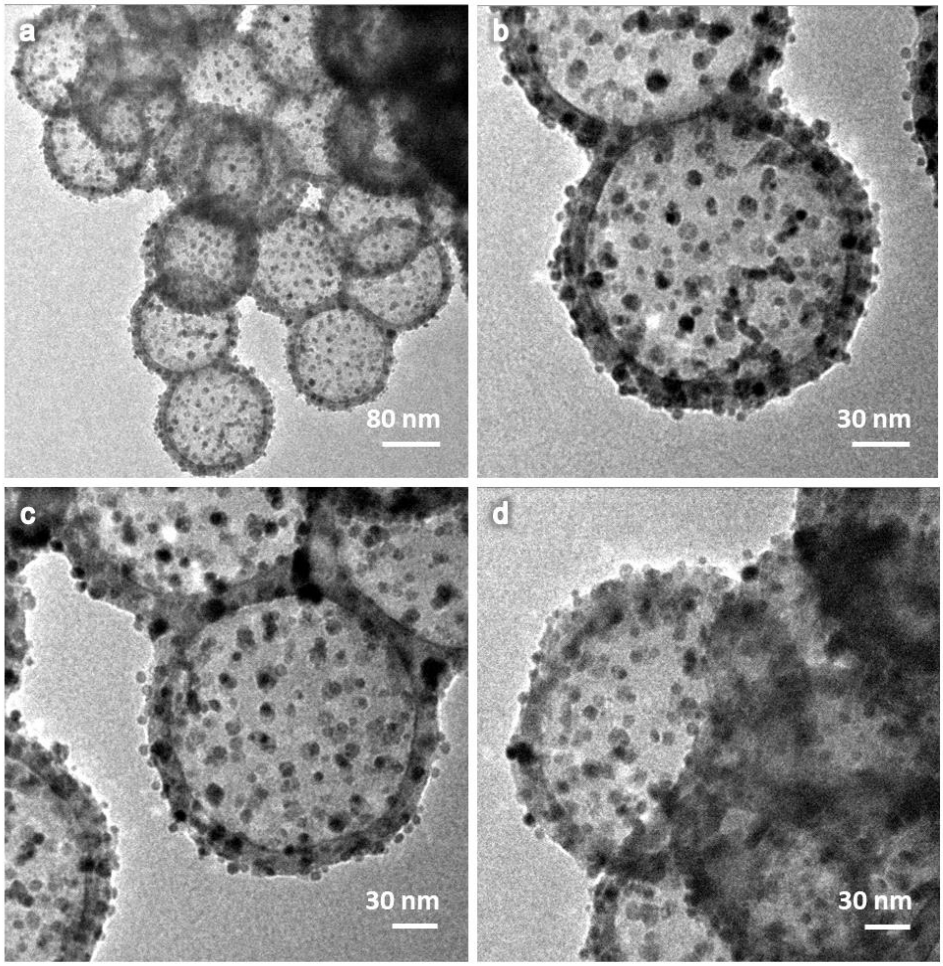

Figure S22. Representative TEM images of $NiPd/SiO_2$ hollow spheres prepared by galvanic replacement with 100 µL of PVP. This sample was prepared using fully reduced Ni/SiO_2 (prepared by H_2 reduction of NiSiO for 6 h at 650 °C) as a precursor.

Comment: Due to the difference in reduction potential, Ni NPs achieved from H_2 reduction of NiSiO hollow spheres could be used to facilitate Pd deposition via galvanic replacement reaction. To achieve that, partially reduced sample (500 °C and 4 h by H_2) was dispersed in ethanol and mixed with Pd solution. Based on above TEM images, it is revealed that such Pd deposition via galvanic replacement will lead to increase in particle size. However, this could be prevented by addition of PVP. The PXRD pattern and EDX mappings suggest the formation of NiPd bimetallic alloy NPs. When fully reduced Ni/SiO_2 sample (H_2 reduction for 650 °C, 6 h) was used, the growth in crystal size could not be inhibited using PVP.

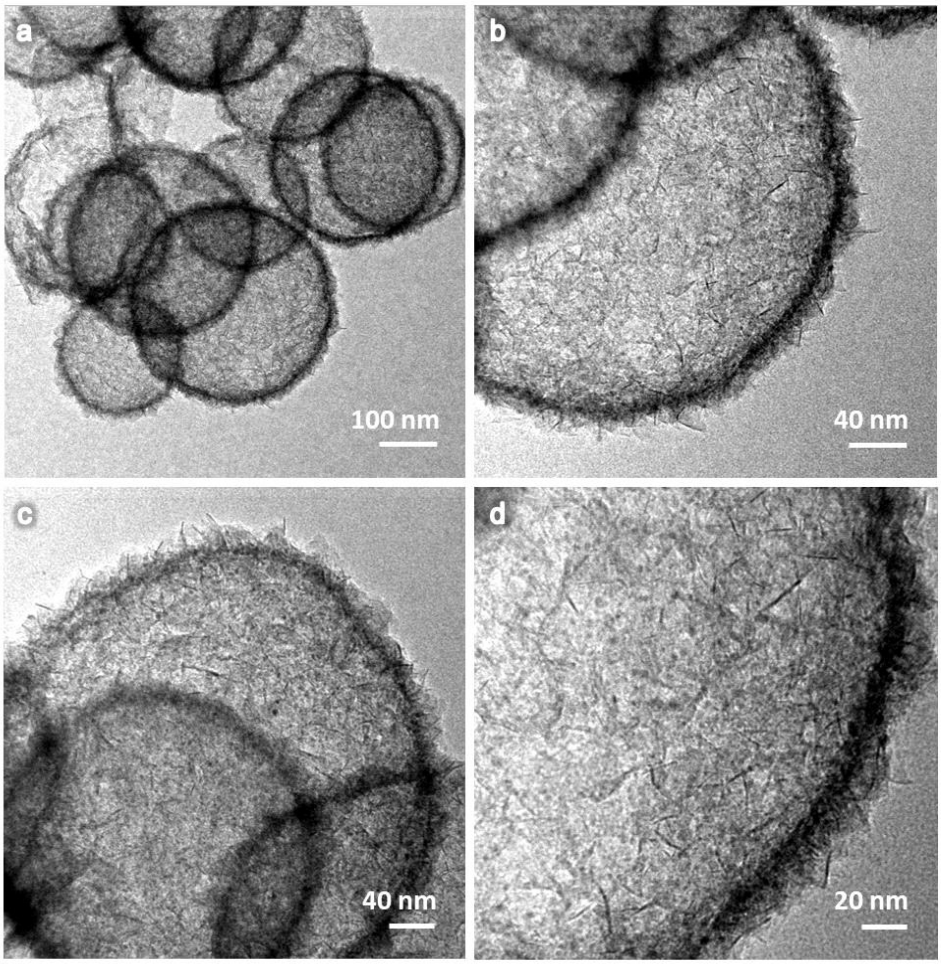

Figure S23. Representative TEM images of NiPd/NiSiO@a_mNi-MOF-74 hollow spheres.

Comment: Preparation of NiPd/NiSiO@a_mNi-MOF-74 was identical to synthesis of Ni/SiO_2@a_mNi-MOF-74, except that NiPd/NiSiO was used as a precursor instead of Ni/SiO_2.

Supporting Table:

Table S1. Estimation of weight percentages for Ni NPs and a_mNi-MOF-74 in different samples.

Sample	Final wt % of sample after TGA calcination	Ni NPs wt % (x)	a_mNi-MOF-74 wt % (y)	Total Ni wt %	Total Ni wt % measured from EDX
Ni/SiO_2@a_mNi-MOF-74 (4h)	97.8	15.6	12.3	20.2	20.1
Ni/SiO_2@a_mNi-MOF-74 (12h)	84.6	5.44	32.1	17.4	18.1
Ni/SiO_2@a_mNi-MOF-74 (16h)	81.9	3.38	36.2	16.8	18.0

Comment: MOF weight percentage in the overall structure was calculated from TGA data. Based on ICP-OES measurement, amount of Ni in Ni/SiO_2 sample was 21.8 wt%. These Ni NPs were then partially oxidized and converted to a_mNi-MOF-74. It is assumed that this a_mNi-MOF-74 follows the same Ni_2DOBDC stoichiometric ratio as crystalline Ni-MOF-74.

The entire Ni/SiO_2@a_mNi-MOF-74 structure could be divided into 3 components, x wt% of Ni NPs, y wt% of a_mNi-MOF-74 and (100–x–y) wt% of SiO_2. As a_mNi-MOF-74 has a chemical formula of Ni_2DOBDC, Ni in a_mNi-MOF-74 is $\frac{58.7\times2}{58.7\times2+198.1}$y wt% (i.e., 0.372y wt%) while $\frac{198.1}{58.7\times2+198.1}$y wt% (i.e., 0.628*y* wt%) is for the organic linker DOBDC.

Assume there is no Ni leaching to solution occurred during MOF synthesis, and the overall amount of Ni and SiO_2 should follow 21.8:78.2 ratio as measured from Ni/SiO_2 sample. Total Ni amount is the sum of Ni NPs and Ni in a_mNi-MOF-74 (x + 0.372y). Total silica amount is the total catalyst weight except the weight of Ni NPs and a_mNi-MOF-74 (100 − x − y). Thus, the following eq. 1 could be constructed,

$$\frac{x + 0.372y}{100 - x - y} = \frac{21.8}{78.2} \qquad (1)$$

During the calcination in air, two reactions occurred. One is nickel oxidation which results in the increase of weight. When Ni is oxidized to NiO, its chemical weight is increased from 58.7 to (58.7+16). Given the total Ni amount is (x + 0.372y), weight increase due to Ni oxidation is then ($\frac{16}{58.7}$(x + 0.372y)). The other reaction is linker decomposition which results in the weight reduction. When the organic linker decomposes, it will become gaseous product and leave the system. Thus, all weight of organic (0.628y) linker needs to be subtracted. Combining these two, we could construct a formula correlating the final weight of sample after TGA calcination with weight percent of Ni NPs (x) and a_mNi-MOF-74 (y) as below,

$$\text{Final wt\% of sample after TGA calcination} = 100 + \frac{16}{58.7}(x + 0.372y) - 0.628y \quad (2)$$

This value, on the other hand, could be directly measured from TGA. In this case, we are comparing the wt% measured at 200 °C and 900 °C and final wt% of sample after TGA calcination (as stated in Table S1) is calculated as $\frac{\text{wt\% of sample at 900°C}}{\text{wt\% of sample at 200°C}}$. The starting point is chosen at 200 °C instead of room temperature as we would like to exclude any weight loss prior due to the loss of adsorbed solvent and ambient gas/vapor. Also, decomposition of organic linker has not started at this temperature. The end point temperature is taken as 900 °C at which we assume all organic linker has decomposed and left the system and all Ni content has been oxidized to NiO.

Taking Ni/SiO_2@a_mNi-MOF-74 (12h) as an example, the wt% of this sample at 200 °C is measured to be 93.6 wt%. At T = 900 °C, the wt% of this sample dropped to 79.1 wt%. The final wt% of Ni/SiO_2@a_mNi-MOF-74 (12h) sample after TGA calcination is then calculated as $\frac{79.1}{93.5} =$ 84.6 wt%.

Substituting the calculated values of final wt% of sample after TGA calcination to equation (2) and solving equations (1) and (2) simultaneously, we could calculate the weight percent of Ni NPs (x) and a_mNi-MOF-74 (y) in each sample, as listed in Table S1.

This calculated total Ni wt % agrees well with the Ni wt % measured from EDX mappings. Thus, we believe that Ni leaching during the formation process is negligible and the Ni distribution based on TGA measurements are accurate.